JOURNAL OF AGRICULTURAL AND FOOD CHEMISTRY

Article

pubs.acs.org/JAFC

Isolation, Structural Elucidation, MS Profiling, and Evaluation of Triglyceride Accumulation Inhibitory Effects of Benzophenone *C*-Glucosides from Leaves of *Mangifera indica* L.

Yi Zhang,[†] Lifeng Han,[†] Dandan Ge,[‡] Xuefeng Liu,[‡] Erwei Liu,[†] Chunhua Wu,[†] Xiumei Gao,[†,‡] and Tao Wang*[,†,‡]

[†]Tianjin State Key Laboratory of Modern Chinese Medicine, 312 Anshanxi Road, Nankai District, Tianjin, 300193, China

[‡]Institute of Traditional Chinese Medicine, Tianjin University of Traditional Chinese Medicine, 312 Anshanxi Road, Nankai District, Tianjin, 300193, China

ABSTRACT: Seventy percent ethanol−water extract from the leaves of *Mangifera indica* L. (Anacardiaceae) was found to show an inhibitory effect on triglyceride (TG) accumulation in 3T3-L1 cells. From the active fraction, six new benzophenone *C*-glucosides, foliamangiferosides A_3 (**1**), A_4 (**2**), C_4 (**3**), C_5 (**4**), C_6 (**5**), and C_7 (**6**) together with 11 known benzophenone *C*-glucosides (**7**−**17**) were obtained. In this paper, isolation, structure elucidation (**1**−**6**), and MS fragment cleavage pathways of all 17 isolates were studied. **1**−**6** showed inhibitory effects on TG and free fatty acid accumulation in 3T3-L1 cells at 10 μM.

KEYWORDS: *Mangifera indica, benzophenone C-glucosides, triglyceride accumulation inhibition, MS fragment cleavage pathways*

INTRODUCTION

Mango tree (*Mangifera indica* L.) belongs to the family Anacardiaceae and is a fruit tree distributed throughout tropical zone. Mango tree leaves have been used as an antitussive in certain Chinese regions.[1] Several xanthone *C*-glycosides, such as mangiferin, gallotannins, and benzophenones, have been isolated from mango tree leaves.[2,3] Including our previous study,[4] benzophenones are reported to have a variety of pharmacological activities, such as antidiabetic,[5] antiulcerogenic action,[6] and antimicrobial.[7]

Our previous studies reported 11 benzophenone *C*-glycosides from mango tree leaves which showed potent inhibitory effects on triglyceride accumulation in 3T3-L1 cells.[4] We further investigated the mass spectrum (MS) fragmentation pathways for rapid identification of benzophenone *C*-glycosides from the extract. On the basis of this method, six new benzophenone *C*-glycosides were found and isolated.

This paper reports the isolation, structure elucidation, bioactivity of the six new compounds, foliamangiferosides A3 (**1**), A4 (**2**), C4 (**3**), C5 (**4**), C6 (**5**), and C7 (**6**), and the MS fragment cleavage rules of benzophenone *C*-glycosides. These results could be further used for rapid profiling the constituents of the extract from mango leaves Chart 1.

RESULTS AND DISCUSSION

Isolation and Structure Elucidation. The dried leaves of *M. indica* were finely cut and extracted with 70% ethanol−water under reflux. Evaporation of the solvent under reduced pressure provided a 70% ethanol−water extract (23.26%). The 70% ethanol−water extract was partitioned into an EtOAc−H_2O (1:1, v/v) mixture to furnish an EtOAc-soluble fraction (6.51%) and an aqueous phase. The EtOAc-soluble fraction was subjected to normal- and reversed-phase column chromatographies and finally HPLC to give new compounds **1** (0.0026%), **2** (0.0241%), **3** (0.0082%), **4** (0.0077%), **5** (0.0088%), and **6** (0.0067%). In addition, 4/5 volume of the aqueous phase was concentrated to 2 L under reduced pressure. The supernatant was further subjected to D101 resin column chromatography (H_2O → 95% EtOH) to give the water- and 95% EtOH-eluted fractions (6.40% and 4.14%, respectively). Eleven known compounds (**7**−**17**) were obtained from the 95% EtOH-eluted fractions as descried methods previously and identified as foliamangiferosides A (**7**), A_1 (**8**), A_2 (**9**), B (**10**), C_1 (**11**), C_2 (**12**), C_3 (**13**), iriflophenone-3-*C*-β-glucoside (**14**), iriflophenone-3-*C*-(2-*O*-*p*-hydroxybenzoyl)-β-D-glucopyranoside (**15**), maclurin-3-*C*-β-D-glucoside (**16**), and mangiferin (**17**) on the basis of chemical and physicochemical evidence or by comparison of their physical data ($[\alpha]_D$, IR, ^{1}H NMR, ^{13}C NMR, MS] with reported values.[4,8]

Foliamangiferoside A_3 (**1**) was obtained as a pale yellow amorphous powder with negative optical rotation ($[\alpha]^{25}_D$ −191.4°, MeOH). Its IR spectrum showed absorptions due to hydroxyl (3294 cm^{-1}), unsaturated carboxyl (1713 cm^{-1}), and aromatic ring (1622, 1609, 1593, 1514, and 1444 cm^{-1}). The molecular formula $C_{34}H_{30}O_{14}$ of **1** was established on the basis of HR-ESI-Q-TOF-MS at *m*/*z* 661.1578 $[M - H]^-$ and 685.1531 $[M + Na]^+$. The ^{1}H (CD_3OD), ^{13}C (CD_3OD, Table 1), and various kinds of 2D NMR spectra (^{1}H−^{1}H COSY, HMQC, HMBC, and NOESY) indicated that there were a 2,4′,6-trihydroxy-4-methoxybenzophenone aglycon [δ_H 7.70 (2H, d, *J* = 8.0 Hz, H-2′,6′), 6.83 (2H, d, *J* = 8.0 Hz, H-3′,5′), 5.84 (1H, s, H-5), 3.56 (3H, s, 4-OC*H*$_3$); δ_C 198.0 (C-7), 56.2 (4-OCH$_3$)], two *p*-hydroxybenzoyl moiety [δ_H 7.80 (2H, d, *J* = 8.4 Hz, H-2‴,6‴), 6.80 (2H, d, *J* = 8.4 Hz, H-3‴,5‴), δ_C 166.9 (C-7‴), and δ_H 7.78 (2H, d, *J* = 8.4 Hz, H-2⁗,6⁗), 6.74 (2H, d, *J* = 8.4 Hz, H-3⁗,5⁗), δ_C 168.0 (C-7⁗)], together with a *C*-β-D-glucopyranosyl moiety

Received: December 10, 2012
Revised: January 31, 2013
Accepted: January 31, 2013
Published: January 31, 2013

Chart 1. Compounds (1−17) Obtained from the Extract of Mango Leaves

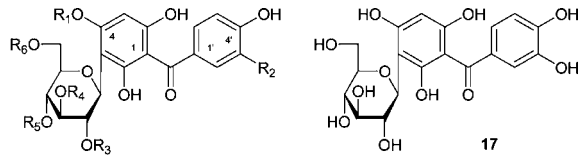

	R_1	R_2	R_3	R_4	R_5	R_6
Foliamangiferoside A_3 (**1**):	CH_3	H	(*a*)	H	H	(*a*)
Foliamangiferoside A_4 (**2**):	CH_3	H	(*b*)	H	H	H
Foliamangiferoside C_4 (**3**):	H	H	(*b*)	H	H	(*a*)
Foliamangiferoside C_5 (**4**):	H	H	(*a*)	H	(*b*)	H
Foliamangiferoside C_6 (**5**):	H	H	(*a*)	(*b*)	H	H
Foliamangiferoside C_7 (**6**):	H	H	H	H	H	(*c*)
Foliamangiferoside A (**7**):	CH_3	H	H	H	H	H
Foliamangiferoside A_1 (**8**):	CH_3	H	(*a*)	H	H	H
Foliamangiferoside A_2 (**9**):	CH_3	H	H	H	H	(*a*)
Foliamangiferoside B (**10**):	CH_3	OCH_3	H	H	H	H
Foliamangiferoside C_1 (**11**):	H	H	H	H	H	(*a*)
Foliamangiferoside C_2 (**12**):	H	H	(*a*)	H	H	(*a*)
Foliamangiferoside C_3 (**13**):	H	H	H	H	H	(*b*)
Iriflophenone-3-*C*-*β*-glucoside (**14**):	H	H	H	H	H	H
(**15**):	H	H	(*a*)	H	H	H
Maclurin-3-*C*-*β*-D-glucoside (**16**):	H	OH	H	H	H	H

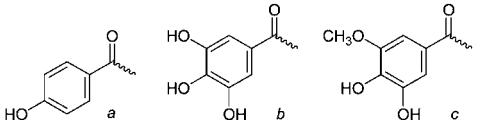

[δ_H 5.22 (1H, d, J = 10.0 Hz, H-1″); δ_C 79.9 (C-5″), 76.9 (C-3″), 74.9 (C-1″), 74.3 (C-2″), 71.3 (C-4″), 64.1 (C-6″)].[4] In the ^{1}H−^{1}H COSY experiment, the correlations between δ_H 5.22 (H-1″) and δ_H 5.46 (1H, dd, J = 10.0, 9.2 Hz, H-2″), δ_H 5.46 and δ_H 3.83 (1H, dd, J = 9.2, 9.2 Hz, H-3″), δ_H 3.83 and δ_H 3.72 (1H, dd, J = 9.2, 9.2 Hz, H-4″), δ_H 3.72 and δ_H 3.81 (1H, m, H-5″), and δ_H 3.81 and δ_H [4.63 (1H, dd, J = 11.6, 4.0 Hz), 4.52 (1H, dd, J = 11.6, 2.0 Hz), H_2-6″] were observed. On the basis of above-mentioned evidence, the presence of the *C*-*β*-D-glucopyranosyl part was clarified. On the other hand, protons of the 2″- and 6″-positions [δ_H 5.46 (H-2″); 4.63, 4.52 (H_2-6″)] resonated at lower fields than those of foliamangiferoside A_1 [δ_H 3.88 (H-2″); 3.84, 3.71 (H_2-6″)] obtained from this plant, which indicated that the two *p*-hydroxybenzoyl moieties linked with the 2″- and 6″-positions, respectively. Furthermore, in the HMBC experiment of **1**, long-range correlations were observed between δ_H 5.22 (H-1″) and δ_C 161.8 (C-4), 158.9 (C-2), and 103.3 (C-3), δ_H 5.46 (H-2″) and δ_C 166.9 (C-7‴), δ_H 6.80 (H-3‴,5‴) and δ_C 166.9 (C-7‴), δ_H 4.62, 4.53 (H_2-6″) and δ_C 168.0 (C-7‴′), and δ_H 6.74 (H-3‴′,5‴′) and δ_C 168.0 (C-7‴′). Then the locations of the *p*-hydroxybenzoyl moiety and glucosyl C−C linkage were clarified. Consequently, foliamangiferoside A_3 was determined as 2,4′,6-trihydroxy-4-methoxy benzophenone-3-*C*-(2,6-bis-*O*-*p*-hydroxybenzoyl)-*β*-D-glucopyranoside (**1**).

Foliamangiferoside A_4 (**2**) was isolated as a pale yellow powder and exhibited a negative optical rotation ([α]$^{25}_D$ −174.7°, MeOH). The molecular formula, $C_{27}H_{26}O_{14}$ of **2** was determined by HR-ESI-Q-TOF-MS with m/z 573.1262 $[M - H]^-$ and 597.1220 $[M + Na]^+$. The ^{1}H (CD_3OD), ^{13}C (CD_3OD, Table 1) and various kinds of 2D NMR spectra suggested that the aglycon of **2** was 2,4′,6-trihydroxy-4-methoxybenzophenone [δ_H 7.72 (2H, d, J = 7.6 Hz, H-2′,6′), 6.80 (2H, d, J = 7.6 Hz, H-3′,5′), 5.85 (1H, s, H-5), 3.60 (3H, s, 4-O*CH*$_3$); δ_C 198.2 (C-7), 56.2 (4-O*CH*$_3$)], too. Furthermore, there were one *C*-*β*-D-glucopyranosyl moiety [δ_H 5.11 (1H, d, J = 9.6 Hz, H-1″); δ_C 82.8 (C-5″), 77.3 (C-3″), 74.7 (C-1″), 74.4 (C-2″), 71.4 (C-4″), 62.2 (C-6″)], and one galloyl group [δ_H 7.01 (2H, s, H-2‴,6‴); δ_C 167.2 (C-7‴), 146.2 (C-3‴,5‴), 139.6 (C-4‴), 121.5 (C-1‴), and 110.3 (C-2‴,6‴)] in **2**. The linkage positions of *C*-*β*-D-glucopyranosyl and galloyl moieties with 2,4′,6-trihydroxy-4-methoxybenzophenone were determined by HMBC experiment. In the HMBC experiment of **2**, long-range correlations were observed between δ_H 5.11 (H-1″) and δ_C 161.8 (C-4), 158.7 (C-2), and 103.5 (C-3); δ_H 5.42 (1H, dd, J = 9.6, 8.8 Hz, H-2″) and δ_C 167.2 (C-7‴); δ_H 7.01 (H-3‴,5‴) and δ_C 167.2 (C-7‴). On the basis of above-mentioned evidence, the structure of foliamangiferoside A_4 was determined as 2,4′,6-trihydroxy-4-methoxy benzophenone-3-*C*-(2-*O*-galloyl)-*β*-D-glucopyranoside (**2**). See Figure 1.

Foliamangiferoside C_4 (**3**) was obtained as a pale yellow amorphous powder with negative optical rotation ([α]$^{25}_D$ −134.8°, MeOH). HR-ESI-Q-TOF-MS revealed the molecular formula of **3** to be $C_{33}H_{28}O_{16}$. The IR spectrum showed absorption bands at 3354 and 1698 cm^{-1}, ascribable to hydroxyl and unsaturated carboxyl and 1608, 1584, 1515, and 1447 cm^{-1} for the aromatic ring. ^{1}H (CD_3OD) and ^{13}C NMR (CD_3OD, Table 1) spectra of **3** showed the presence of the following partial structures: one 2,4,4′,6-tetrahydroxy benzophenone aglycon part [δ_H 7.59 (2H, d, J = 8.4 Hz, H-2′,6′), 6.76 (2H, d, J = 8.4 Hz, H-3′,5′),

Table 1. ^{13}C NMR (100 MHz, CD_3OD, δ) Data of Compounds 1−6

	1	2	3	4	5	6
1	109.1	109.2	107.4	107.1	107.4	107.5
2	158.9	158.7	161.4	161.3	161.1	160.8
3	103.3	103.5	102.7	102.8	102.6	104.4
4	161.8	161.8	161.4	162.7	162.7	162.9
5	92.1	92.0	96.3	95.5	96.0	96.1
6	161.0	160.4	162.6	161.3	161.1	160.6
7	198.0	198.2	198.9	199.0	198.9	198.7
1′	132.6	132.5	133.3	132.8	132.8	134.0
2′	133.3	133.4	132.9	133.2	133.1	133.0
3′	115.7	115.7	115.5	115.4	115.5	115.5
4′	163.2	163.2	162.8	162.7	162.8	162.5
5′	115.7	115.7	115.5	115.4	115.5	115.5
6′	133.3	133.4	132.9	133.2	133.1	132.0
1″	74.9	74.7	74.7	74.5	74.4	76.9
2″	74.3	74.4	74.2	74.3	72.1	73.9
3″	76.9	77.3	77.4	75.8	78.7	79.5
4″	71.3	71.4	71.5	72.6	69.7	71.3
5″	79.9	82.8	80.0	81.2	83.0	79.7
6″	64.1	62.2	64.3	62.2	62.1	64.4
OCH_3	56.2	56.2				
1‴	121.8	121.5	121.1	122.2	121.8	121.1
2‴	132.87	110.3	110.4	133.0	132.9	106.0
3‴	116.0	146.2	146.2	115.9	115.9	149.1
4‴	163.4	139.6	139.6	163.3	163.4	140.7
5‴	116.0	146.2	146.2	115.9	115.9	146.3
6‴	132.87	110.3	110.4	133.0	132.9	112.0
7‴	166.9	167.2	167.5	167.3	167.0	168.1
OCH_3						56.7
1‴′	122.2		121.9	121.1	121.3	121.8
2‴′	132.93		132.9	110.4	110.4	132.9
3‴′	116.2		116.2	146.5	146.3	116.2
4‴′	163.5		163.6	140.1	139.8	163.4
5‴′	116.2		116.2	146.5	146.3	116.2
6‴′	132.93		132.9	110.4	110.4	132.9
7‴′	168.0		168.0	167.7	168.0	168.1

dx.doi.org/10.1021/jf305256w | J. Agric. Food Chem. 2013, 61, 1884−1895

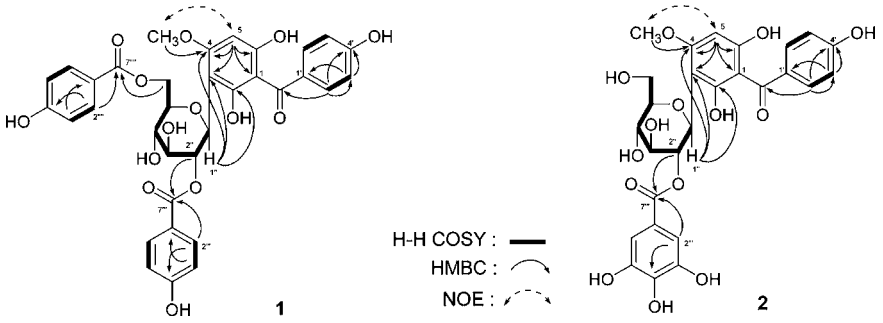

Figure 1. Key $^{1}H-^{1}H$ COSY, HMBC, and NOE correlations of compounds **1** and **2**.

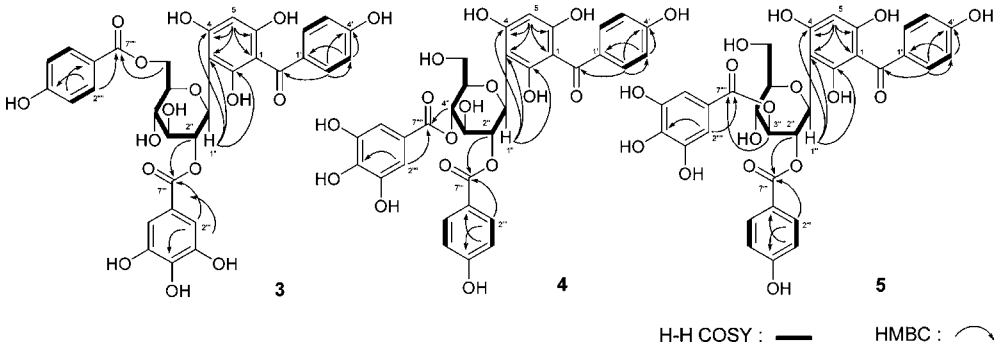

Figure 2. Key $^{1}H-^{1}H$ COSY and HMBC correlations of compounds **3**, **4**, and **5**.

5.80 (1H, s, H-5); δ_C 198.9 (C-7)], one galloyl group [δ_H 7.04 (2H, s, H-2‴,6‴); δ_C 167.5 (C-7‴), 146.2 (C-3‴,5‴), 139.6 (C-4‴), 121.1 (C-1‴), and 110.4 (C-2‴,6‴)], one *p*-hydroxybenzoyl moiety [δ_H 7.83 (2H, d, J = 7.8 Hz, H-2‴′,6‴′), 6.78 (2H, d, J = 7.8 Hz, H-3‴′,5‴′); δ_C168.0 (C-7‴′)], together with one *C*-*β*-D-glucopyranosyl moiety [δ_H 5.20 (1H, d, J = 9.6 Hz, H-1″); δ_C 80.0 (C-5″), 77.4 (C-3″), 74.7 (C-1″), 74.2 (C-2″), 71.5 (C-4″), 64.3 (C-6″)]. The $^{1}H-^{1}H$ COSY experiment indicated the presence of a partial structure written in the bold line shown in Figure 2. Linkage of *C*-*β*-D-glucopyranosyl moiety in **3** was clarified by the HMBC experiment, which showed long-range correlations observed between the 1″-proton and the 2-, 3-, and 4-carbons (δ_C 161.4, 102.7, and 161.4) (Figure 2). On the other hand, the observed long-range correlations between δ_H 5.56 (1H, dd, J = 9.6, 9.2 Hz, H-2″) and δ_C 167.5 (C-7‴), δ_H 7.04 (2H, H-2‴,6‴) and δ_C 167.5 (C-7‴), δ_H [4.62 (1H, dd, J = 12.0, 3.6 Hz), 4.54 (1H, br d, ca. J = 12 Hz), H_2-6″] and δ_C 168.0 (C-7‴′), and δ_H 7.83 (2H, d, J = 7.8 Hz, H-2‴′,6‴′) and δ_C 168.0 (C-7‴′) suggested that the galloyl and *p*-hydroxybenzoyl moieties linked with the 2- and 6″-position, respectively. Then foliamangiferoside C_4 was determined as 2,4,4′,6-tetrahydroxy benzophenone-3-*C*-(2-*O*-galloyl)-(6-*O*-*p*-hydroxybenzoyl)-*β*-D-glucopyranoside (**3**).

Foliamangiferosides C_5 (**4**) and C_6 (**5**) were obtained as amorphous powders with negative optical rotation (**4** $[\alpha]^{25}_D$ −81.3°; **5** $[\alpha]^{25}_D$ −12.6°, both in MeOH, respectively). The same molecular formula, $C_{33}H_{28}O_{16}$, for both **4** and **5** were determined individually from positive- and negative-ion HR-ESI-Q-TOF-MS. ^{1}H (CD_3OD) and ^{13}C NMR (CD_3OD, Table 1) spectra of **4** and **5** indicated the presence of the following functions: one 2,4′,4,6-tetrahydroxybenzophenone aglycon part {**4** [δ_H 7.80 (2H, d, J = 7.6 Hz, H-2′,6′), 6.72 (2H, d, J = 7.6 Hz, H-3′,5′), 5.84 (1H, s, H-5); δ_C 199.0 (C-7)]; **5** [7.68 (2H, d, J = 7.6 Hz, H-2′,6′), 6.74 (2H, d, J = 7.6 Hz, H-3′,5′); 5.90 (1H, s, H-5); δ_C 198.9 (C-7)], one *p*-hydroxybenzoyl moiety {[**4** δ_H 7.80 (2H, d, J = 7.6 Hz, H-2‴,6‴), 6.66 (2H, d, J = 7.6 Hz, H-3‴,5‴); δ_C 167.3 (C-7‴)]; **5** δ_H 7.68 (2H, d, J = 7.6 Hz, H-2‴,6‴), 6.66 (2H, d, J = 7.6 Hz, H-3‴,5‴); δ_C 167.0 (C-7‴)]}, one galloyl group {**4** [δ_H 7.13 (2H, s, H-2‴′,6‴′); δ_C 167.7 (C-7‴′), 146.5 (C-3‴′,5‴′), 140.1 (C-4‴′), 121.1 (C-1‴′), and 110.4 (C-2‴′,6‴′)]; **5** [δ_H 7.03 (2H, s, H-2‴′,6‴′); δ_C 168.0 (C-7‴′), 146.3 (C-3‴′,5‴′), 139.8 (C-4‴′), 121.3 (C-1‴′), and 110.4 (C-2‴′,6‴′)]], together with one *C*-*β*-D-glucopyranosyl moiety {**4** [δ_H 5.25 (1H, d, J = 9.6 Hz, H-1″); δ_C 81.2 (C-5″), 75.8 (C-3″), 74.5 (C-1″), 74.3 (C-2″), 72.6 (C-4″), 62.2 (C-6″)]; **5** [δ_H 5.29 (1H, d, J = 10.0 Hz, H-1″); δ_C 83.0 (C-5″), 78.7 (C-3″), 74.4 (C-1″), 72.1 (C-2″), 69.7 (C-4″), 62.1 (C-6″)]}, respectively. In the HMBC experiment, long-range correlations were observed between H-1″ and C-2, -3, and -4 [**4** between δ_H 5.25 (H-1″) and δ_C 162.7 (C-4), 161.3 (C-2), and 102.8 (C-3); **5** between δ_H 5.29 (H-1″) and δ_C 162.7 (C-4), 161.1 (C-2), and 102.6 (C-3)] and H-2″ and the carbonyl carbon of the *p*-hydroxybenzoyl group [**4** between δ_H 5.75 (1H, dd, J = 9.6, 9.6 Hz, H-2″) and δ_C 167.3 (C-7‴); **5** between δ_H 5.81 (1H, dd, J = 10.0, 9.6 Hz, H-2″), and δ_C δ_C 167.3 (C-7‴)], whereas long-range correlation between δ_H 5.26 (1H, dd, J = 9.6, 9.6 Hz, H-4″) and δ_C 167.7 (C-7‴′) and δ_H 5.50 (1H, dd, J = 9.6, 9.2 Hz, H-3″) and δ_C 167.7 (C-7‴′) was observed in the HMBC experiment for **4** and **5**, respectively. On the basis of the above-mentioned evidence, the structures of **4** and **5** were clarified to be 2,4,4′,6-tetrahydroxy benzophenone-3-*C*-(2-*O*-*p*-hydroxybenzoyl)-(4-*O*-galloyl)-*β*-D-glucopyranoside and 2,4,4′,6-tetrahydroxy benzophenone-3-*C*-(2-*O*-*p*-hydroxybenzoyl)-(3-*O*-galloyl)-*β*-D-glucopyranoside, respectively.

Foliamangiferoside C_7 (**6**), $[\alpha]^{25}_D$ −34.1° (MeOH), was also obtained as a pale yellow amorphous powder. The molecular formula, $C_{27}H_{26}O_{14}$, of **6** was determined from the positive- and negative-ion HR-ESI-Q-TOF-MS. Proton and carbon signals in ^{1}H (CD_3OD) and ^{13}C NMR (Table 1) spectra indicated that the aglycon of **6** was the same as compounds **3**−**5**, 2,4,4′,

dx.doi.org/10.1021/jf305256w | J. Agric. Food Chem. 2013, 61, 1884−1895

6-tetrahydroxy benzophenone [δ_H 7.61 (2H, d, J = 8.4 Hz, H-2′,6′), 6.74 (2H, d, J = 8.4 Hz, H-3′,5′), 5.97 (1H, s, H-5); δ_C 198.7 (C-7)], except for it there was an unsymmetrical tetrasubstituted benzyl group [δ_H 7.18 (1H, d, J = 2.0 Hz, H-6‴), 7.10 (1H, d, J = 2.0 Hz, H-2‴)], one methoxy group [δ_H 3.74 (3H, s, 3‴-OCH_3); 56.7 (3‴-OCH_3)], and one *C*-β-D-glucopyranosyl moiety [δ_H 4.96 (1H, d, J = 10.0 Hz, H-1″); δ_C 79.7 (C-5″), 79.5 (C-3″), 76.9 (C-1″), 73.9 (C-2″), 71.3 (C-4″), 64.4 (C-6″)]. The ^{1}H−^{1}H COSY experiment indicated the presence of a partial structure written in the bold line shown in Figure 3. Furthermore, in the HMBC

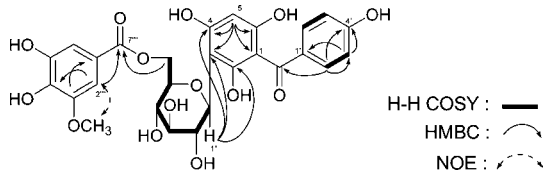

Figure 3. Key ^{1}H−^{1}H COSY, HMBC, and NOE correlations of compound **6**.

experiment of **6**, long-range correlations between the following protons and carbons were observed: δ_H 4.96 (H-1″) and δ_C 162.9 (C-4), 160.8 (C-2), and 104.4 (C-3); δ_H [4.61 (1H, dd, J = 11.6, 3.6 Hz), 4.45 (1H, dd, J = 11.6, 1.6 Hz), H_2-6″] and δ_C 168.1 (C-7‴); δ_H 7.18 (H-6‴) and δ_C 168.1 (C-7‴), 146.3 (C-5‴), 140.7 (C-4‴), and 121.1 (C-1‴); δ_H 7.10 (H-2‴) and δ_C 168.1 (C-7‴), 149.1 (C-3‴), 140.7 (C-4‴), and 121.1 (C-1‴); δ_H 3.74 (3‴-OCH_3) and δ_C 149.2 (C-3‴). In addition, in the NOESY experiment on **6**, the correlation between δ_H 7.10 (H-2‴) and δ_H 3.74 (3‴-OCH_3) was observed. On the basis of the above-mentioned evidence, foliamangiferoside C_7 was determined as 2,4,4′,6-tetrahydroxybenzophenone-3-*C*-(6-*O*-(3-methoxygalloyl)-β-D-glucopyranoside (**6**).

MS Fragment Cleavage Pathways. Q-TOF-MS spectra were detected in both positive- and negative-ion modes. The major ion species generated were $[M + H]^+$ and $[M - H]^-$ in positive- and negative-ion modes, respectively. Although a little higher sensitivity was achieved in positive mode, the $[M - H]^-$ ion was selected for MS/MS analysis due to $[M + H]^+$ ion producing a complex array of low-abundance ions for MS/MS analysis which were difficult to interpret.

The nomenclature (foliamangiferoside C_5 as an example, Figure 4) commonly used for flavonoid was adopted to denote

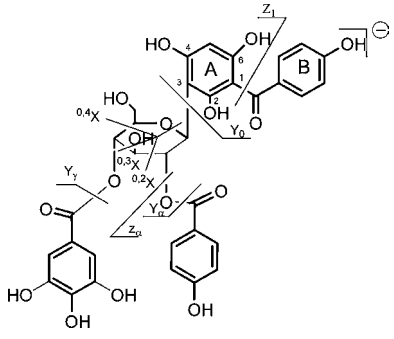

Figure 4. Cleavage nomenclature of foliamangiferoside C_5 (**4**).

the fragment ions to assist structural elucidation. The ions retaining the charge on the main core structures were termed as Y, Z (glycosidic or substituent cleavages), and X (cross-ring cleavages). The Y_0 ion was produced via loss of a sugar residue (with/without substituent group), and the Y_α, Y_β, Y_γ, and Y_δ ions were formed via elimination of the substituent groups from C-2, C-3, C-4, and C-6 of the saccharide, respectively. Cross-ring cleavage ions were designated by superscript numbers, indicating the two bonds cleaved.

Figure 5a presents the full-scan mass spectrum of compound **14** in negative-ion mode. ESI-Q-TOF-MS analysis of **14** yielded a $[M - H]^-$ ion at m/z 407.0993 (Table 2). In the MS/MS spectrum of $[M - H]^-$ (Figure 5b), fragment ions at m/z 317.0695, 287.0593, 245.0497, 193.0164, 167.0369, and 125.0260 corresponded to ^{0,3}X, ^{0,2}X, Y_0, ^{0,2}X − 92 Da − H_2, ^{0,2}X − 120 Da, and Y_0 − 120 Da (Figure 6). A similar diagnostic cleavage pattern was observed in the MS/MS spectra of compounds **7**, **10**, and **16** (see Table 3).

As to compound **17**, the xanthone in the reference which we obtained from the extract of mango leaves, the base peak of the MS/MS spectrum was 331.0435 corresponding to ^{0,3}X. Similarly, ^{0,2}X and Y_0 ions were observed at m/z 301.0331 and 259.0227.

Compound **11** showed the $[M - H]^-$ ion at m/z 527.1224 which corresponded to $C_{26}H_{23}O_{12}$. In the MS/MS spectra, fragment ions at m/z 407.0956 and 389.0830 showed the presence of the *p*-hydroxybenzoyl moiety (loss of 120 and 138 Da). Other characteristic fragment ions for the *C*-glycosidic compound, such as ^{0,3}X, ^{0,2}X, Y_0, ^{0,2}X − 92 Da − H_2, ^{0,2}X − 120 Da and Y_0 − 120 Da, were similar with compound **14**. The difference between compounds **9** and **11** was that **9** contained CH_3O− at the C-4 position of aglycone which resulted in it being 14 Da higher than **11**. Therefore, m/z 541.1336 was observed for the $[M - H]^-$ ion in negative full-scan mode. The presence of the *p*-hydroxybenzoyl moiety (loss of 120 and 138 Da), ^{0,3}X, ^{0,2}X, Y_0, ^{0,2}X − 92 Da − H_2, and ^{0,2}X − 120 Da were all found (see Table 3).

Compound **13** gave a $[M - H]^-$ ion at m/z 559.1115, and the presence of a galloyl moiety was clear due to fragment ions at m/z 407.0947 (loss of 152 Da) and 389.0851 (loss of 170 Da) besides the presence of other characteristic fragmentation of a *C*-glycosidic compound. Fragment ion at m/z 439.0850 was found which corresponded to Z_1 ion. It is worth noting that M − ^{0,2}X and M − ^{0,3}X ions were observed at m/z 271.0435 and 241.0329 (see Figure 7).

As to compound **6**, the $[M - H]^-$ ion was obtained at m/z 573.1268 in negative MS spectra and the ^{0,3}X, ^{0,2}X, Y_0, ^{0,2}X − 92 Da − H_2, ^{0,2}X − 120 Da, and Y_0 − 120 Da were observed at m/z 317.0687, 287.0583, 245.0472, 193.0156, 167.0362, and 125.0254 in MS/MS spectra, respectively. Similar to **13**, the M − ^{0,2}X and M − ^{0,3}X ions (14 Da higher than **13**) were observed at m/z 285.0630 and 255.0525.

Compound **15** was an isomer of **11**; besides the diagnostic ions for the presence of *p*-hydroxybenzoyl moiety at m/z 407.0955 (loss of 120 Da) and 389.0842 (loss of 138 Da) and other characteristic ions for *C*-glycoside, the fragment ions at m/z 269.0433 and 311.0583 which corresponded to ^{0,2}X − 120 Da − H_2O and ^{0,4}X − 138 Da were observed, respectively. According to Tables 2 and 3, compounds **8** and **9** were also isomers and the characteristic fragment ions were all observed (14 Da higer than compound **15**).

Compound **2** yielded the $[M - H]^-$ ion at m/z 573.1263 in the ESI-Q-TOF-MS spectrum. In the MS/MS spectrum of $[M - H]^-$, the characteristic ions for the presence of galloyl moiety at m/z 421.1163 and 403.1050 which corresponded to the loss of 152 and 170 Da were obtained, respectively.

dx.doi.org/10.1021/jf305256w | J. Agric. Food Chem. 2013, 61, 1884−1895

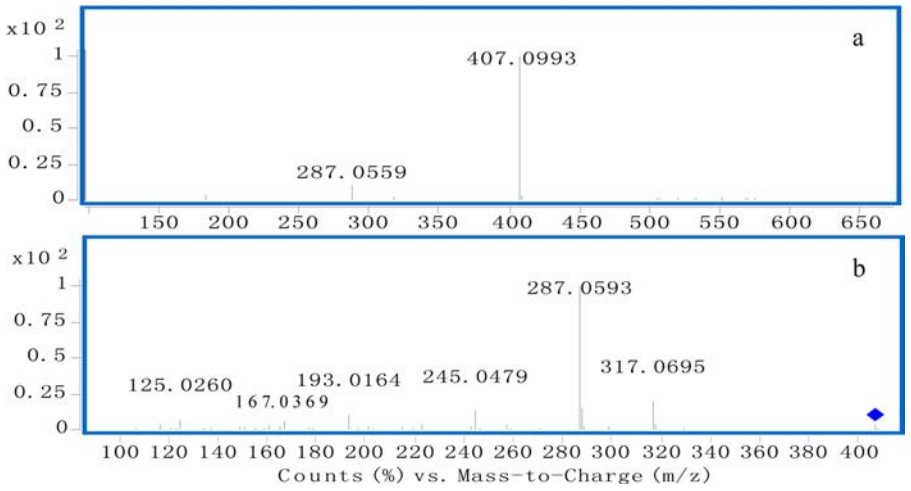

Figure 5. ESI-MS and MS/MS spectra of compound **14** (a) -ESI-MS; (b) MS/MS of the $[M - H]^-$ ion.

Table 2. ESI-TOF-MS Data of Compounds 1−17 Identified from the Extract of Mango Leaves

peaks	RT (min)	formula	selected ion	*m/z* experimental	*m/z* calculated	error (ppm)
1	3.86	$C_{19}H_{20}O_{11}$	$[M - H]^-$	423.0937	423.0933	−0.97
2	6.23	$C_{19}H_{20}O_{10}$	$[M - H]^-$	407.0993	407.0984	−2.36
3	8.49	$C_{19}H_{18}O_{11}$	$[M - H]^-$	421.0784	421.0776	−1.92
4	9.30	$C_{20}H_{22}O_{10}$	$[M - H]^-$	421.1145	421.1140	−1.12
5	10.11	$C_{21}H_{24}O_{11}$	$[M - H]^-$	451.1245	451.1246	+0.22
6	14.38	$C_{27}H_{26}O_{14}$	$[M - H]^-$	573.1264	573.1250	−2.52
7	14.61	$C_{26}H_{24}O_{14}$	$[M - H]^-$	559.1114	559.1093	−3.70
8	16.78	$C_{26}H_{24}O_{12}$	$[M - H]^-$	527.1203	527.1195	−1.51
9	18.27	$C_{27}H_{26}O_{14}$	$[M - H]^-$	573.1225	573.1250	+4.41
10	20.39	$C_{26}H_{24}O_{12}$	$[M - H]^-$	527.1200	527.1195	−0.90
11	20.39	$C_{27}H_{26}O_{12}$	$[M - H]^-$	541.1352	541.1351	−0.13
12	20.55	$C_{33}H_{28}O_{16}$	$[M - H]^-$	679.1323	679.1305	−2.74
13	21.81	$C_{33}H_{28}O_{16}$	$[M - H]^-$	679.1328	679.1305	−3.41
14	22.17	$C_{27}H_{26}O_{12}$	$[M - H]^-$	541.1336	541.1351	+2.97
15	22.60	$C_{33}H_{28}O_{16}$	$[M - H]^-$	679.1314	679.1305	−1.36
16	25.23	$C_{33}H_{28}O_{14}$	$[M - H]^-$	647.1428	647.1406	−3.36
17	27.48	$C_{34}H_{30}O_{14}$	$[M - H]^-$	661.1578	661.1563	−2.25

The fragment ions at *m/z* 301.0738, 283.0633, 193.0162, 169.0161, and 125.0256 corresponded to $^{0,2}X - 152$ Da, $^{0,2}X - 152$ Da $- H_2O$, $^{0,2}X - 92$ Da $- 2H$, Z_α, and $Y_0 - 120$ Da.

Compared to **15**, compound **12** contained another *p*-hydroxybenzoyl moiety at the C-6 position of glucose. According to the ESI-Q-TOF-MS spectrum, **12** gave $[M - H]^-$ at *m/z* 647.1416. In the MS/MS spectrum, the fragment ions at *m/z* 527.1211 $[M - H - 120\ Da]^-$, 509.1097 $[M - H - 138\ Da]^-$, 389.0891 $[M - H - 138\ Da - 120\ Da]^-$, and 371.0790 $[M - H - 138\ Da - 138\ Da]^-$ showed the presence of two *p*-hydroxybenzoyl moieties. All other characteristic fragment ions were similar to compound **15**. Similarly, a fragment pathway was observed between compound **1** and **8** (14 Da higher than **12** and **15**, see Table 3).

Figure 8 shows the fragment pathway of compound **3**, the fragment ions at *m/z* 527.1195 $[M - H - 152\ Da]^-$, 509.1079 $[M - H - 170\ Da]^-$, 407.0989 $[M - H - 152\ Da - 120\ Da]^-$, 389.0885 $[M - H - 152\ Da - 138\ Da]^-$, and 371.0776 $[M - H - 170\ Da - 138\ Da]^-$ corresponded to the presence of a *p*-hydroxybenzoyl moiety and a galloyl moiety. Fragment ions at *m/z* 317.0681, 287.0577, 269.0469, 245.0470, 193.0154, 169.0152, 137.0257, and 125.0251 corresponded to $^{0,3}X$, $^{0,2}X$, $^{0,2}X - H_2O$, Y_0, $^{0,2}X - 92$ Da $- 2H$, Z_α, Z_δ, and $Y_0 - 120$ Da.

Compounds **4** and **5** were isomers of **3**; however, MS/MS spectra were different from each other. According to Figure 9, we could deduce that when the C-2 position of glucose was substituted with either a *p*-hydroxybenzoyl residue or a galloyl residue, the bond would be easy to cleave at first. Beside the characteristic fragment ions similar to **3**, compounds **4** and **5** had a significant fragment ion at *m/z* 271 which corresponded to M − H − 120 Da $- ^{0,2}X$ ions (see Figures 10 and 11).

Our previous study reported that benzophenone *C*-glucosides from mango tree leaves showed an inhibitory effect on TG accumulation in 3T3-L1 adipocytes.[4] The mechanism of their lipid homeostasis activity is possibly exerted through the AMP-activated protein kinase (AMPK) pathway by up-regulation of AMPK and down-regulation of sterol regulatory element-binding protein 1c (SREBP1c), hormone-sensitive lipase (HSL), and fatty acid synthase (FAS).

3T3-L1 preadipocytes were treated with compounds **1**−**6** at doses of 10 μM. In this concentration, there were no treatment-related changes in cell viability (MTT method, data not shown). In compounds **1** and **2**, the 4-methoxy benzophenone *C*-glucosides showed weaker inhibitory effects on TG and FFA accumulation compared with **3**−**6** (Figure 12). This tendency agrees with the structure−activity relationship study results on

Table 3. MS/MS Data of Compounds 1−17 Identified from the Extract of Mango Leaves

peaks	(−) ESI-MS *m/z*	MS/MS (*m/z*, %)	compounds
1	423.0937 $[M - H]^-$	333.0593 (18), 303.0491 (100), 261.0390 (4), 193.0126 (65), 167.0333 (7), 125.0229 (7)	**16**
2	407.0993 $[M - H]^-$	317.0695 (20), 287.0593 (100), 245.0497 (13), 193.0164 (10), 167.0369 (5), 125.0260 (7)	**14**
3	421.0784 $[M - H]^-$	331.0435 (100), 301.0331 (40), 259.0227 (15)	**17**
4	421.1145 $[M - H]^-$	331.0847 (2), 301.0751 (100), 259.0617 (1), 207.0324 (52), 181.0525 (1), 139.0417 (1)	**7**
5	451.1245 $[M - H]^-$	361.0954 (3), 331.0853 (100), 289.0721 (1), 207.0320 (27), 181.0521 (1), 139.0412 (1)	**10**
6	573.1264 $[M - H]^-$	421.1163 (21), 403.1050 (3), 301.0738 (1), 283.0633 (1), 193.0162 (2), 169.0161 (100), 125.0256 (8)	**2**
7	559.1114 $[M - H]^-$	439.0850 (7), 407.0947 (2), 389.0851 (3), 317.0639 (38), 287.0534 (100), 271.0435 (95), 245.0434 (6), 241.0329 (20), 193.0121 (3), 169.0122 (15), 167.0329 (7), 125.0229 (4)	**13**
8	527.1203 $[M - H]^-$	407.0955 (3), 389.0842 (8), 317.0640 (5), 311.0583 (20), 287.0539 (18), 269.0433 (100), 245.0434 (1)	**15**
9	573.1225 $[M - H]^-$	453.1050 (1), 407.0991 (1), 389.0897 (1), 317.0687 (26), 287.0583 (100), 285.0630 (4), 255.0525 (2), 245.0472 (4), 193.0156 (3), 167.0362 (6), 125.0254 (2)	**6**
10	527.1200 $[M - H]^-$	407.0956 (1), 389.0830 (1), 317.0639 (22), 287.0538 (100), 245.0429 (6), 193.0116 (4), 167.0326 (3), 125.0227 (3)	**11**
11	541.1352 $[M - H]^-$	421.1086 (5), 403.0997 (31), 325.0684 (1), 301.0685 (4), 283.0580 (100), 259.0572 (1)	**8**
12	679.1323 $[M - H]^-$	559.1101 (7), 541.1005 (20), 521.1203 (16), 509.1104 (4), 421.0788 (8), 407.0981 (4), 389.0901 (100), 371.0794 (40), 311.0585 (57), 299.0586 (40), 287.0593 (1), 271.0484 (40), 269.0482 (85), 211.0270 (7), 169.0160 (60), 137.0284 (2), 125.0260 (6)	**5**
13	679.1328 $[M - H]^-$	585.1090 (3), 541.0984 (12), 421.0789 (9), 389.0891 (12), 371.0782 (8), 317.0672 (4), 311.0583 (7), 287.0580 (3), 271.0479 (100), 269.0474 (40), 211.0265 (17), 169.0154 (11), 137.0157 (1), 125.0247 (2)	**4**
14	541.1336 $[M - H]^-$	421.1099 (3), 403.0992 (13), 331.0785 (5), 301.0688 (100), 259.0588 (1), 207.0274 (14), 181.0597(10)	**9**
15	679.1314 $[M - H]^-$	527.1195(11), 509.1079 (4), 407.0989 (3), 389.0885 (3), 371.0776 (3), 317.0681 (20), 287.0577 (100), 269.0469 (46), 245.0470 (20), 193.0154 (12), 169.0152 (30), 137.0257 (1), 125.0251(4)	**3**
16	647.1428 $[M - H]^-$	527.1211 (1), 509.1097 (10), 389.0891 (3), 371.0790 (3), 317.0683(3), 311.0586 (16), 287.0583 (3), 269.0479 (100), 245.0494 (1)	**12**
17	661.1578 $[M - H]^-$	541.1298 (3), 523.1202 (24), 403.1003 (1), 385.0904 (2), 301.0688 (4), 283.0589 (72), 239.0540 (100), 179.0332 (7), 137.0226 (5)	**1**

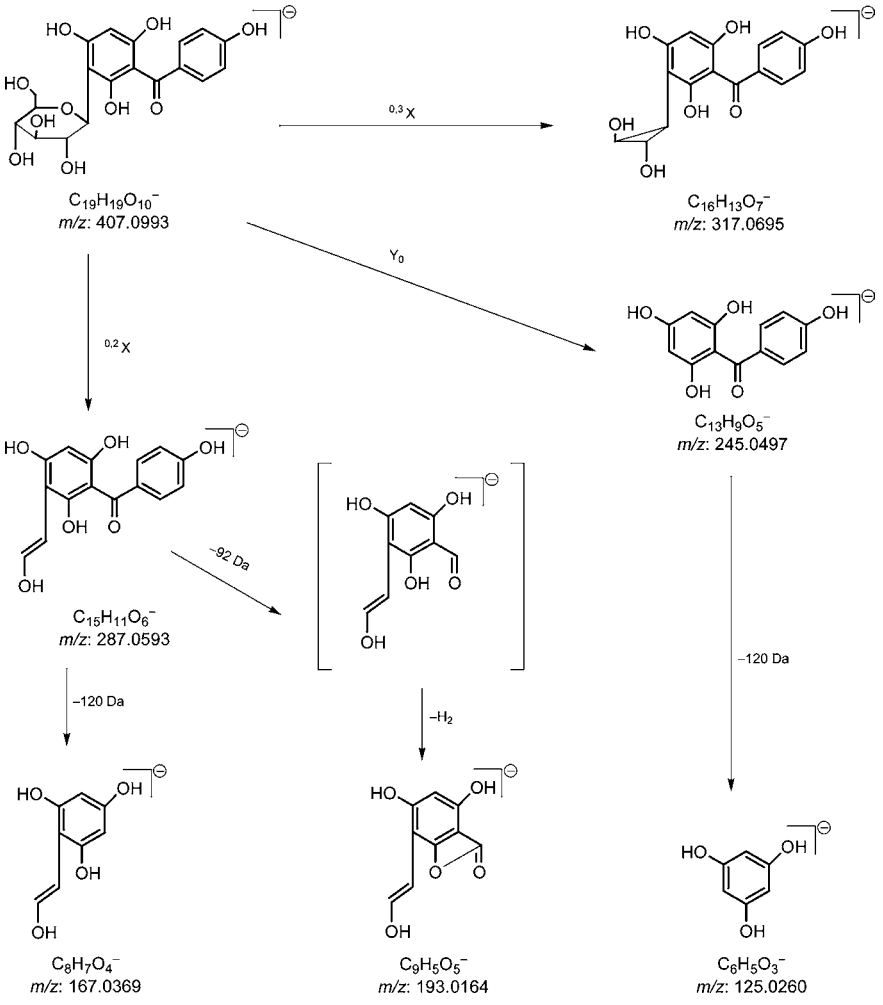

Figure 6. Cleavage pattern of compound **14**.

dx.doi.org/10.1021/jf305256w | *J. Agric. Food Chem.* 2013, 61, 1884−1895

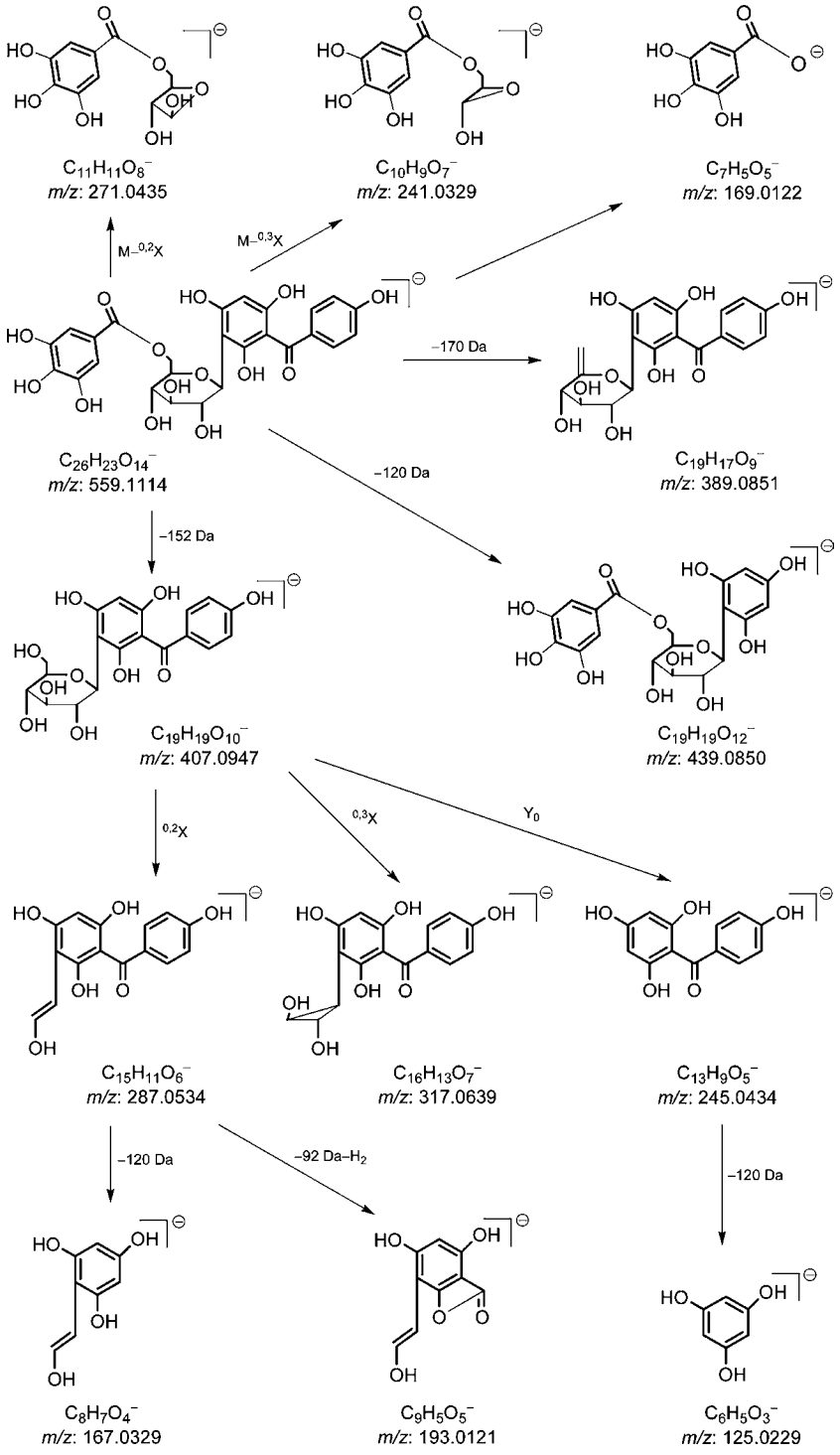

Figure 7. Cleavage pattern of compound **13**.

7−**17**.[4] Compared with **1**, TG levels of compounds **5** and **6** were significantly reduced ($P < 0.05$).

AMPK plays a key role in cellular energy homeostasis.[9] The AMPK pathway is regarded as a potential therapeutic target for type 2 diabetes, obesity, and metabolic syndrome. AMPK activator, such as Metaformin, can increase energy production and switches off pathways which consume energy,[10] leads to reduce energy storage, and increases energy production to reestablish normal cellular energy balance. Up-regulated phosphorylation of the AMPK (*p*-AMPK) level indicated stimulation of fatty acid metabolism occurred.[11] Activation of AMPK in adipocytes leads to a decreased fatty acid uptake and decreased triglyceride synthesis via inhibition of lipogenic genes expression, such as SREBP 1c, FAS, and HSL.[12]

As shown in Figure 13, compounds **1**−**6** significantly increased the AMPK gene expression. Compounds **2**−**6** significantly reduced SREBP1c expression. HSL was down-regulated by **4**−**6**, and FAS was down-regulated by **2**−**6**. Combined with previous studies, this result indicated that the effect of benzophenone *C*-glucosides from mango tree leaves on the lipid accumulation inhibitory effect is mediated, at least in part, through the AMPK signaling pathway.

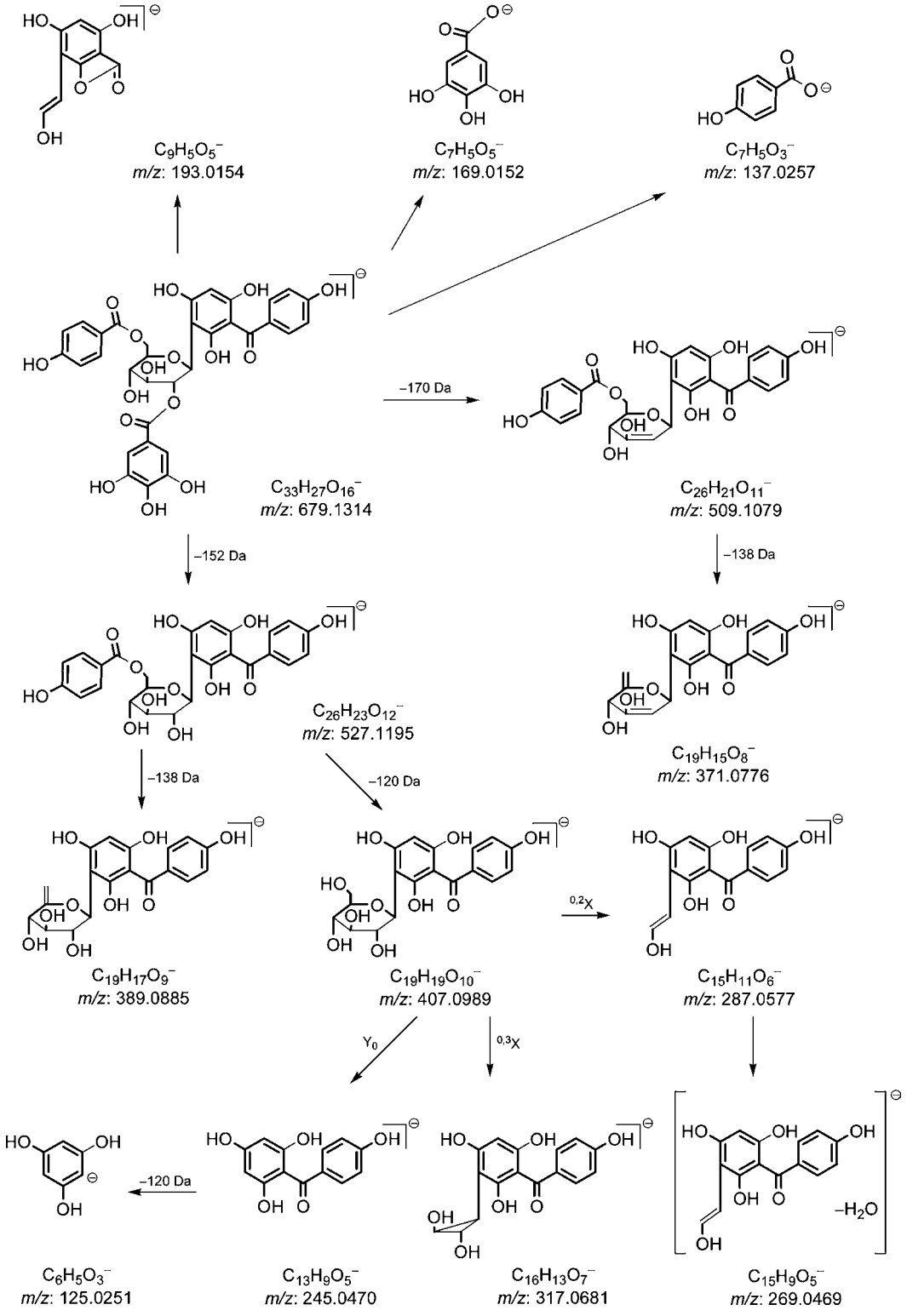

Figure 8. Cleavage pattern of compound **3**.

EXPERIMENTAL SECTION

General Experimental Procedures. The following instruments were used to obtain physical data: Optical rotations were measured on a Rudolph Autopol IV automatic polarimeter (l = 50 mm), IR were recorded on a Varian 640-IR FT-IR spectrophotometer, and UV spectra were recorded on a Varian Cary 50 UV−vis spectrophotometer. ^{1}H and ^{13}C NMR spectra were determined on a Varian 400MR spectrometer at 400 MHz for ^{1}H and 100 MHz for ^{13}C NMR, with tetramethylsilane (TMS) as an internal standard. Positive- and negative-ion HR-ESI-Q-TOF-MS were recorded on an Aglient 6520 Q-TOF mass spectrometer (Agilent Corp., Santa Clara, CA, USA).

The following experimental conditions were used for chromatography: A macroporous synthetic resin (D101) was purchased from Haiguang Chemical Co., Ltd. (Tianjin, China). Silica gel CC were obtained from Qingdao Haiyang Chemical Co., Ltd. (48−75 μm, Qingdao, China). Sephadex LH-20 (Ge Healthcare Bio-Sciences, Swiss) was used to purify the total benzophenone C-glucosides from

dx.doi.org/10.1021/jf305256w | J. Agric. Food Chem. 2013, 61, 1884−1895

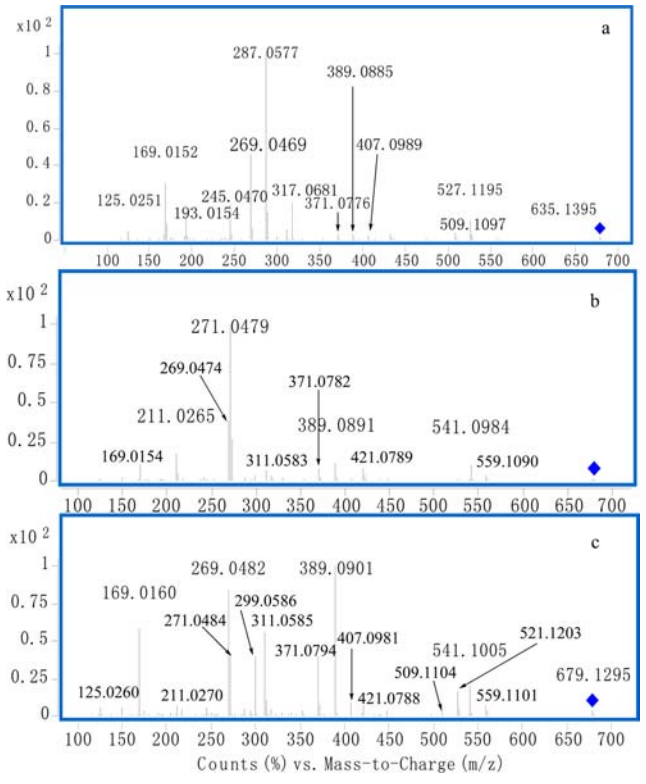

Figure 9. (−) ESI-MS/MS spectrum of compounds **3** (a), **4** (b), and **5** (c).

the whole residue. HPLC was performed on ODS (Cosmosil 5C18-MS-II, Tokyo, Japan; Φ = 20 mm, *L* = 250 mm, flow rate 9.0 mL/min), and the eluate was monitored with a UV detector (Shimadzu RID-10A UV−vis, Japan). Precoated TLC plates with silica gel GF_{254} (Tianjin Silida Technology Co., Ltd., Tianjin, China) were used to detect the purity of isolate achieved by spraying with 10% aqueous H_2SO_4−EtOH followed by heating.

Plant Material. In the present study, mango leaves were collected from Zhejiang Province, China, and identified by Dr. Tianxiang Li at Tianjin University of TCM as *M. indica* L. Voucher specimen was deposited at the Academy of Traditional Chinese Medicine of Tianjin University of TCM.

Extraction and Isolation. The dried leaves of *M. indica* L. were finely cut and extracted with 70% ethanol−water under reflux. Evaporation of the solvent under reduced pressure provided a 70% ethanol−water extract (23.26%). The 70% ethanol−water extract was partitioned into an EtOAc−H_2O (1:1, v/v) mixture to furnish an EtOAc-soluble fraction (6.51%). The EtOAc layer (120.0 g) was subjected to the SiO_2 gel column chromatography [$CHCl_3$ → $CHCl_3$−MeOH (100:1 → 5:1, v/v) → MeOH] to furnish seven fractions [fraction 1 (0.8 g), fraction 2 (2.2 g), fraction 3 (1.0 g), fraction 4 (0.5 g), fraction 5 (0.2 g), fraction 6 (73.0 g), fraction 7 (46.0 g)]. Fraction 6 (60.0 g) was further separated by SiO_2 gel column chromatography [$CHCl_3$−MeOH (100:1 → 100:3 → 100:4 → 100:7 → 10:1, v/v) → MeOH], and eight fractions [fraction 6-1 (0.1 g), fraction 6-2 (10.4 g), fraction 6-3 (1.3 g), fraction 6-4 (3.4 g), fraction 6-5 (2.7 g), fraction 6-6 (0.7 g), fraction 6-7 (6.8 g), fraction 6-8 (30.5 g)] were obtained. Fraction 6-7 (5.0 g) was isolated with reversed-phase silica gel column chromatography [MeOH−H_2O (0:100 → 10:90 → 30:70 → 50:50 → 70:30 → 80:20 → 90:10 → 100:0, v/v)] to give 10 fractions [fraction 6-7-1 (379.2 mg), fraction 6-7-2 (240.0 mg), fraction 6-7-3 (893.5 mg), fraction 6-7-4 (333.9 mg), fraction 6-7-5 (382.2 mg), fraction 6-7-6 (158.6 mg), fraction 6-7-7 (100.9 mg), fraction 6-7-8 (136.3 mg), fraction 6-7-9 (115.0 mg), fraction 6-7-10 (1720.8 mg)]. Fraction 6-7-7 (100.9 mg) was purified by HPLC [MeOH−H_2O (45:55, v/v) + 1% HAc] and further [MeOH−H_2O (40:60, v/v) + 1% HAc] to afford foliamangiferoside A_3 (**1**, 29.2 mg, 0.0026%). Fraction 6-8 (25.0 g) was subjected to normal-phase silica gel column chromatography [$CHCl_3$−MeOH−H_2O (10:3:1 → 7:3:1, v/v/v, lower layer) → MeOH] to afford 7 fractions [fraction 6-8-1 (0.3 g), fraction 6-8-2 (1.1 g), fraction 6-8-3 (2.6 g), fraction 6-8-4 (5.5 g), fraction 6-8-5 (6.7 g), fraction 6-8-6 (0.7 g), fraction 6-8-7 (6.5 g)]. Fraction 6-8-5 (5.0 g) was subjected to Sephadex LH-20 column chromatography [MeOH] to give 5 fractions [fraction 6-8-5-1 (373.3 mg), fraction 6-8-5-2 (2183.8 mg), fraction 6-8-5-3 (2071.2 mg), fraction 6-8-5-4 (495.6 mg), fraction 6-8-5-5 (47.3 mg)]. Fractions 6-8-5-2 (2183.8 mg) and 6-8-5-3 (2071.2 mg) were isolated by HPLC [MeOH−H_2O (40:60, v/v) +1% HAc] to give foliamangiferosides A_4 (**3**, 64.1 mg, 0.0241%), C_4 (**3**, 23.0 mg, 0.0082%), C_5 (**4**, 21.6 mg, 0.0077%), C_6 (**5**, 24.7 mg, 0.0088%), and C_7 (**6**, 18.8 mg, 0.0067%).

The known compounds **7**−**17** were isolated as descried methods previously and identified by comparison of their physical data ($[\alpha]_D$, IR, ^{1}H NMR, ^{13}C NMR, MS) with reported values.[4,8]

LC-MS Sample Preparation and Reagents. All reference compounds were purified from the extract of mango leaves by the author, and the purity was higher than 95% which was detected by the HPLC-ELSD base on peak area normalization method. Reference solutions were prepared by dissolving each in 50% (v/v) methanol−water (about 1 mg·mL^{-1}) and stored at 4 °C until analysis.

HPLC-grade acetonitrile (Merck KGaA, Darmstadt, Germany) and fomic acid (Tedia, USA) were utilized for UHPLC analysis. Deionized water was purified using a Milli-Q system (Millipore, Bedford, MA, USA). All other chemicals were of analytical grade.

UHPLC-Q-TOF-MS Parameters. UHPLC analyses were performed on an Agilent 1290 UHPLC instrument (Agilent, Waldbronn, Germany) coupled to a binary pump, a diode-array detector, an autosampler, and a column thermostat. Sample was separated on a Waters BEH C18 column (1.7 μm, 150 × 2.1 mm; Waters Technologies). Mobile phase consisted of CH_3CN (solvent B) and H_2O (containing 0.1% HCOOH; solvent A). A gradient program was used according to the following profile: 0−15 min, 8−18% B; 15−30 min, 18−40% B; 31 min increased to 100% B; 31−35 min, 100% B; 40 min decreased to 8% B. The flow rate was 0.3 mL/min, and the column temperature was set at 30 °C.

An Aglient 6520 Q-TOF mass spectrometer (Agilent Corp., Santa Clara, CA, USA) was connected to the Agilent 1290 UHPLC instrument via an ESI interface. Acquisition parameters were as follows: drying gas (N_2) flow rate, 8.0 L/min; temperature, 360 °C; nebulizer, 30 psig; capillary, −4500 V; fragmentor, 175 V; skimmer, 65 V; OCT RF V, 750 V. Mass range recorded *m*/*z* 100−1200. The quasi-molecular ion $[M - H]^-$ of interest in the negative ESI mode MS scan was selected as precursor ion and subjected to Target-MS/MS analyses. The collision energy (CE) was set at 20−25 V.

Foliamangiferoside A_3 (1). Pale yellow powder; $[\alpha]^{25}_D$ −191.4° (*c* = 1.3, MeOH); UV (MeOH) λ_{max} (log ε) 309 (4.08, shoulder), 260 (4.53); IR (KBr) λ_{max} 3294, 2968, 2901, 2839, 1713, 1622, 1609, 1593, 1514, 1444, 1377, 1317, 1275, 1168, 1129, 1083, 998, 850 cm^{-1}; ^{1}H NMR data (400 MHz, CD_3OD) δ 7.80 (2H, d, *J* = 8.4 Hz, H-2‴,6‴), 7.78 (2H, d, *J* = 8.4 Hz, H-2‴′,6‴′), 7.70 (2H, d, *J* = 8.0 Hz, H-2′,6′), 6.83 (2H, d, *J* = 8.0 Hz, H-3′,5′), 6.80 (2H, d, *J* = 8.4 Hz, H-3‴,5‴), 6.74 (2H, d, *J* = 8.4 Hz, H-3‴′,5‴′), 5.84 (1H, s, H-5), 5.46 (1H, dd, *J* = 10.0, 9.2 Hz, H-2″), 5.22 (1H, d, *J* = 10.0 Hz, H-1″), [4.63 (1H, dd, *J* = 11.6, 4.0 Hz), 4.52 (1H, dd, *J* = 11.6, 2.0 Hz), H_2-6″], 3.83 (1H, dd, *J* = 9.2, 9.2 Hz, H-3″), 3.81 (1H, m, H-5″), 3.72 (1H, dd, *J* = 9.2, 9.2 Hz, H-4″), 3.56 (3H, s, 4-OC*H*$_3$); ^{13}C NMR data, see Table 1; positive-ion mode HR-ESI-Q-TOF-MS *m*/*z* 685.1531 (calcd for $C_{34}H_{30}O_{14}Na$ $[M + Na]^+$, 685.1528), negative-ion mode HR-ESI-Q-TOF-MS *m*/*z* 661.1578 (calcd for $C_{34}H_{29}O_{14}$ $[M - H]^-$, 661.1563).

Foliamangiferoside A_4 (2). Pale yellow powder; $[\alpha]^{25}_D$ −174.7° (*c* = 0.4, MeOH); UV (MeOH) λ_{max} (log ε) 285 (4.31); IR (KBr) λ_{max} 3361, 2965, 2832, 1697, 1607, 1582, 1511, 1447, 1373, 1319, 1218, 1165, 1122, 1080, 997, 847 cm^{-1}; ^{1}H NMR data (400 MHz, CD_3OD) δ 7.72 (2H, d, *J* = 7.6 Hz, H-2′,6′), 7.01 (2H, s, H-2‴,6‴), 6.80 (2H, d, *J* = 7.6 Hz, H-3′,5′), 5.85 (1H, s, H-5), 5.42 (1H, dd, *J* = 9.6, 8.8 Hz, H-2″), 5.11 (1H, d, *J* = 9.6 Hz, H-1″), [3.88 (1H, br d, ca. *J* = 12 Hz), 3.77 (1H, dd, *J* = 12.0, 4.8 Hz), H_2-6″], 3.77 (1H, m, H-3″), 3.62

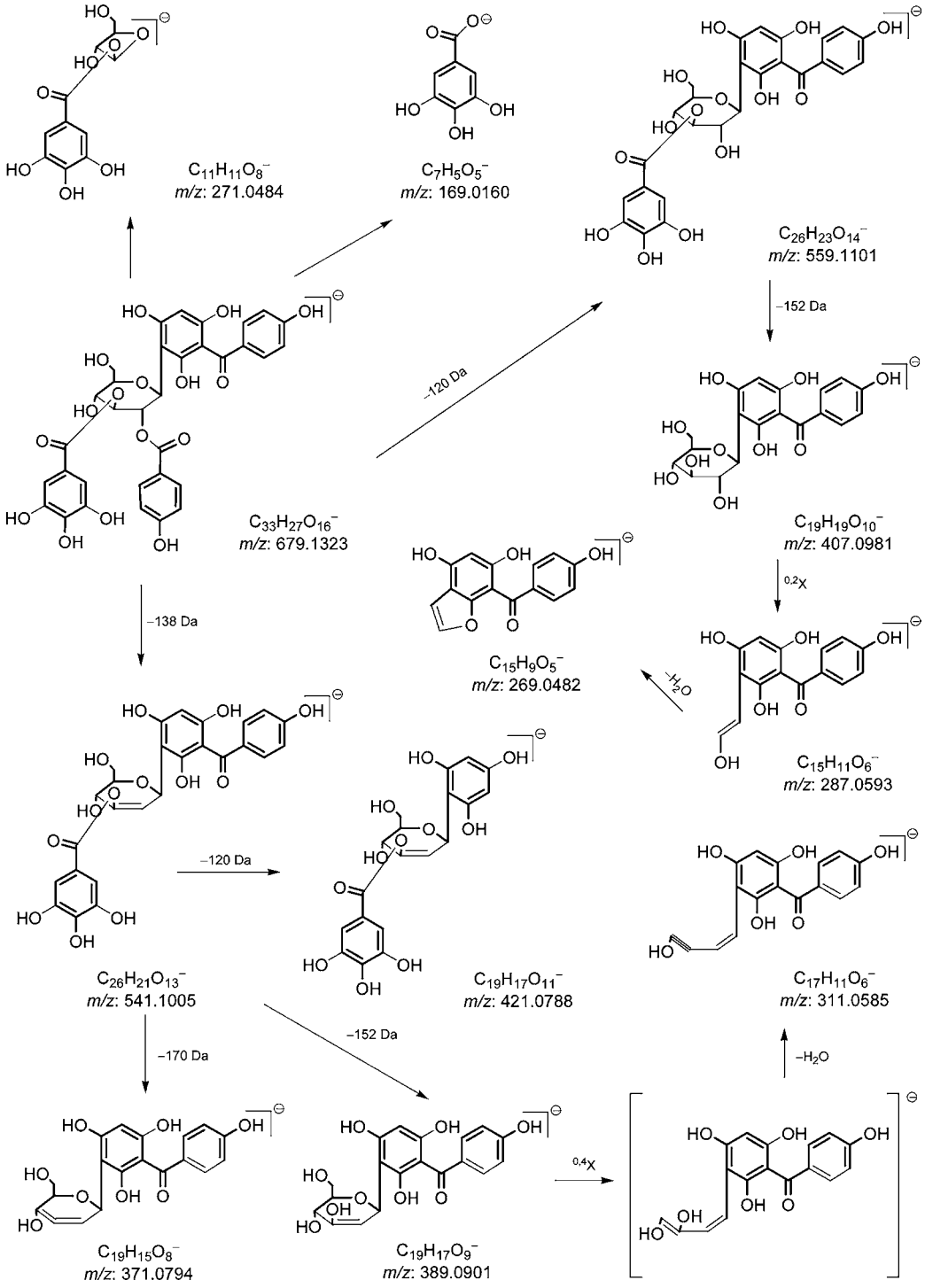

Figure 10. Cleavage pattern of compound **5**.

(1H, dd, J = 9.2, 9.2 Hz, H-4″), 3.60 (3H, s, 4-OCH_3), 3.56 (1H, dd, J = 9.2, 8.8 Hz, H-5″); ^{13}C NMR (100 MHz, CD_3OD) data, see Table 1; positive-ion mode HR-ESI-Q-TOF-MS m/z 597.1220 (calcd for $C_{27}H_{26}O_{14}Na$ $[M + Na]^+$, 597.1215), negative-ion mode HR-ESI-Q-TOF-MS m/z 573.1262 (calcd for $C_{27}H_{25}O_{14}$ $[M - H]^-$, 573.1250).

Foliamangiferoside C_4 (3). Pale yellow powder; $[\alpha]^{25}_D$ −134.8° (c = 0.1, MeOH); UV (MeOH) λ_{max} (log ε) 329 (4.02, shoulder), 269 (4.31); IR (KBr) λ_{max} 3354, 2967, 2835, 1698, 1608, 1584, 1515, 1447, 1383, 1279, 1168, 1122, 1082, 945, 850 cm^{-1}; ^{1}H NMR data (400 MHz, CD_3OD) δ 7.83 (2H, d, J = 7.8 Hz, H-2‴′,6‴′), 7.59 (2H, d, J = 8.4 Hz, H-2′,6′), 7.04 (2H, s, H-2‴,6‴), 6.78 (2H, d, J = 7.8 Hz, H-3‴′,5‴′), 6.76 (2H, d, J = 8.4 Hz, H-3′,5′), 5.80 (1H, s, H-5), 5.56 (1H, dd, J = 9.6, 9.2 Hz, H-2″), 5.20 (1H, d, J = 9.6 Hz, H-1″), [4.62 (1H, dd, J = 12.0, 3.6 Hz), 4.54 (1H, br d, ca. J = 12 Hz), H_2-6″], 3.80 (1H, dd, J = 9.2, 9.2 Hz, H-3″), 3.80 (1H, m, H-5″), 3.72 (1H, dd, J = 9.2, 9.2 Hz, H-4″); ^{13}C NMR (100 MHz, CD_3OD) data, see Table 1; positive-ion mode HR-ESI-Q-TOF-MS m/z 703.1279 (calcd for $C_{33}H_{28}O_{16}Na$ $[M + Na]^+$, 703.1270), negative-ion mode HR-ESI-Q-TOF-MS m/z 679.1323 (calcd for $C_{33}H_{27}O_{16}$ $[M - H]^-$, 679.1305).

Foliamangiferoside C_5 (4). Pale yellow powder; $[\alpha]^{25}_D$ −81.3° (c = 0.2, MeOH); UV (MeOH) λ_{max} (log ε) 339 (3.90, shoulder), 270 (4.30); IR (KBr) λ_{max} 3354, 2967, 2835, 1698, 1608, 1584, 1515, 1447, 1383, 1279, 1168, 1122, 1082, 945, 850 cm^{-1}; ^{1}H NMR data

dx.doi.org/10.1021/jf305256w | J. Agric. Food Chem. 2013, 61, 1884−1895

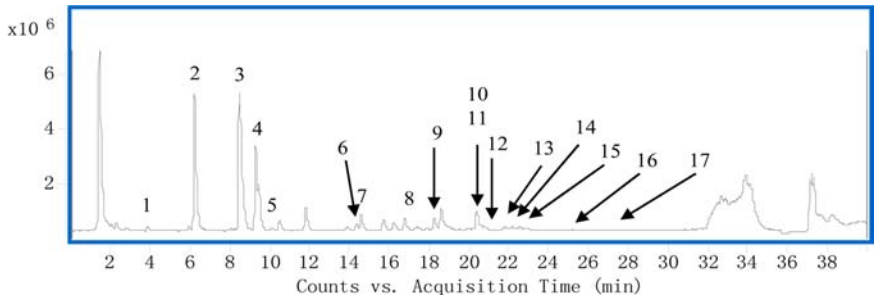

Figure 11. (−) TIC chromatogram of the extract of leaves of *M. indica* L.

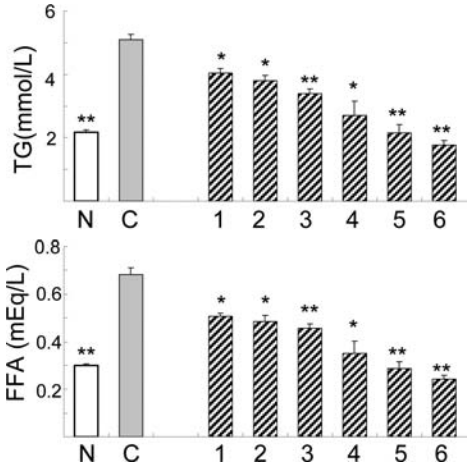

Figure 12. TG and FFA accumulation inhibitory effects of **1**−**6** in mature 3T3-L1 cells. Fourteen days after induction of differentiation, cells were lysis by omni ruptor and determined with the TG kit and NEFA kit according to the protocols provided by the manufacturer. N, normal group; C, control group; number, treated with 10 μM compound. Values represent the mean ± SD of six determinations. *P < 0.05; **P < 0.01 vs control group.

(400 MHz, CD_3OD) δ 7.80 (4H, d, J = 7.6 Hz, H-2′,6′, and 2‴,6‴), 7.13 (2H, s, H-2‴′,6‴′), 6.72 (2H, d, J = 7.6 Hz, H-3′,5′), 6.66 (2H, d, J = 7.6 Hz, H-3‴,5‴); 5.84 (1H, s, H-5), 5.75 (1H, dd, J = 9.6, 9.6 Hz, H-2″), 5.26 (1H, dd, J = 9.6, 9.6 Hz, H-4″), 5.25 (1H, d, J = 9.6 Hz, H-1″), 4.09 (1H, dd, J = 9.6, 9.2 Hz, H-3″), 3.80 (1H, m, H-5″), [3.66 (1H, br d, ca. J = 13 Hz), 3.63 (1H, dd, J = 12.8, 5.2 Hz), H_2-6″]; ^{13}C NMR (100 MHz, CD_3OD) data, see Table 1; positive-ion mode HR-ESI-Q-TOF-MS m/z 703.1287 (calcd for $C_{33}H_{28}O_{16}Na$ [M + Na]$^+$, 703.1270), negative-ion mode HR-ESI-Q-TOF-MS m/z 679.1320 (calcd for $C_{33}H_{27}O_{16}$ [M − H]$^-$, 679.1305).

Foliamangiferoside C_6 (5). Pale yellow powder; $[\alpha]^{25}_D$ −12.6° (c = 0.1, MeOH); UV (MeOH) λ_{max} (log ε) 327 (4.12, shoulder), 270 (4.37); IR (KBr) λ_{max} 3359, 2974, 2830, 1704, 1607, 1578, 1513, 1450, 1318, 1274, 1168, 1079, 1011, 849 cm^{-1}; ^{1}H NMR data (400 MHz, CD_3OD) δ 7.68 (4H, d, J = 7.6 Hz, H-2′,6′, and 2‴,6‴), 7.03 (2H, s, H-2‴′,6‴′), 6.74 (2H, d, J = 7.6 Hz, H-3′,5′), 6.66 (2H, d, J = 7.6 Hz, H-3‴,5‴), 5.90 (1H, s, H-5), 5.81 (1H, dd, J = 10.0, 9.6 Hz, H-2″), 5.50 (1H, dd, J = 9.6, 9.2 Hz, H-3″), 5.29 (1H, d, J = 10.0 Hz, H-1″), [3.93 (1H, br d, ca. J = 12 Hz), 3.84 (1H, dd, J = 12.8, 6.0 Hz), H_2-6″]; 3.92 (1H, dd, J = 9.6, 9.2 Hz, H-4″), 3.64 (1H, m, H-5″); ^{13}C NMR (100 MHz, CD_3OD) data, see Table 1; positive-ion mode HR-ESI-Q-TOF-MS m/z 703.1277 (calcd for $C_{33}H_{28}O_{16}Na$ [M + Na]$^+$, 703.1270), negative-ion mode HR-ESI-Q-TOF-MS m/z 679.1315 (calcd for $C_{33}H_{27}O_{16}$ [M − H]$^-$, 679.1305).

Foliamangiferoside C_7 (6). Pale yellow powder; $[\alpha]^{25}_D$ −34.1° (c = 0.1, MeOH); UV (MeOH) λ_{max} (log ε) 327 (3.91, shoulder), 280 (4.15); IR (KBr) λ_{max} 3361, 2970, 2831, 1698, 1608, 1575, 1514, 1454, 1384, 1319, 1272, 1167, 1086, 1012, 848 cm^{-1}; ^{1}H NMR data (400 MHz, CD_3OD) δ 7.61 (2H, d, J = 8.4 Hz, H-2′,6′), 7.18 (1H, d, J = 2.0 Hz, H-6‴), 7.10 (1H, d, J = 2.0 Hz, H-2‴), 6.74 (2H, d, J = 8.4 Hz, H-3′,5′), 5.97 (1H, s, H-5), 4.96 (1H, d, J = 10.0 Hz, H-1″), [4.61 (1H, dd, J = 11.6, 3.6 Hz), 4.45 (1H, dd, J = 11.6, 1.6 Hz), H_2-6″], 3.90 (1H, dd, J = 10.0, 8.8 Hz, H-2″), 3.74 (3H, s, 3‴-OCH_3), 3.71 (1H, m, H-5″), 3.58 (1H, dd, J = 9.2, 8.8 Hz, H-4″), 3.52 (1H, dd, J = 8.8, 8.8 Hz, H-3″); ^{13}C NMR (100 MHz, CD_3OD) data, see Table 1; positive-ion mode HR-ESI-Q-TOF-MS m/z 597.1226 (calcd for $C_{27}H_{26}O_{14}Na$ [M + Na]$^+$, 597.1215), negative-ion mode HR-ESI-Q-TOF-MS m/z 573.1272 (calcd for $C_{27}H_{25}O_{14}$ [M − H]$^-$, 573.1250).

Bioassay. The inhibitory effect on lipid accumulation was assessed in 3T3-L1 cells by measuring intracellular triglyceride (TG) and free fatty acid (FFA) as described previously.[4] Briefly, cells were exposed to

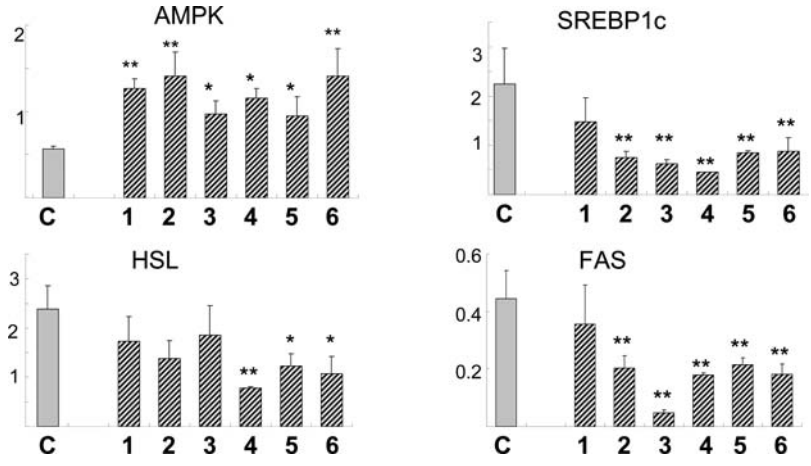

Figure 13. Effects of **1**−**6** on adipogenic relative gene expression in mature 3T3-L1 cells. C, control group; number, treated with 10 μM compound. Values represent the mean ± SD of six determinations. *P < 0.05; **P < 0.01 vs control group.

differentiation medium containing 1 μM dexamethasone, 0.5 mM 3-isobutylmethylxanthine, and 10 μg/mL insulin for 14 days together with 10 μM sample DMSO solution (final DMSO concentration was 0.5%). The amount of intracellular TG and FFA was determined with the Triglycerides kit (BioSino Biotechnology and Science Inc., China) and NEFA-C kit (NEFA C-test wako, Japan) after cell lysis, respectively. TG and NEFA values were corrected by their protein content. Total RNA was isolated from 3T3-L1 adipocytes with TRIzol reagent (Invitrogen, USA). One microgram of RNA was reverse transcribed by the High Capacity cDNA Reverse Transcription Kit (Applied Biosystems, USA) to obtain cDNA according to the protocols provided by the manufacturer. Real-time PCR was performed with an Applied Biosystems 7500 Real-Time PCR System (Applied Biosystems, USA) using Power SYBR Green PCR master mix (Applied Biosystems, USA) according to the protocols provided by the manufacturer. PCR reactions consisted of an initial denaturating cycle at 95 °C for 10 min, followed by 40 amplification cycles: 15 s at 95 °C and 1 min at 60 °C. Primers used were as described previously. Results are presented as levels of expression relative to those of controls after normalization to GADPH using the $2^{-\Delta\Delta CT}$ method. Analysis was carried out in triplicate.

AUTHOR INFORMATION

Corresponding Author

*Tel.: +86 22 5959 6163; Fax: +86 22 5959 6163; E-mail: wangt@263.net.

Funding

Part of this research was supported by the Important Drug Development Fund, Ministry of Science and Technology of China (2012ZX09103201-031), Program for New Century Excellent Talents in University (NCET-10-0958), and Applied Basic and Advanced Research Program of Tianjin (10ZCKFSY09300, 10SYSYJC28900).

Notes

The authors declare no competing financial interest.

REFERENCES

(1) Jiang, Y.; You, X. Y.; Fu, K. L.; Yin, W. L. Effects of Extract from Mangifera indica Leaf on Monosodium Urate Crystal-Induced Gouty Arthritis in Rats. *J. Evidence-Based Complementary Altern. Med.* **2012**, 967573.

(2) Barreto, J. C.; Trevisan, M. T.; Hull, W. E.; Erben, G.; deBrito, E. S.; Pfundstein, B.; Wurtele, G.; Spiegelhalder, B.; Owen, R. W. Characterization and quantitation of polyphenolic compounds in bark, kernel, leaves, and peel of mango (Mangifera indica L.). *J. Agric. Food Chem.* **2008**, *56* (14), 5599−610.

(3) Singh, U. P.; Singh, D. P.; Singh, M.; Maurya, S.; Srivastava, J. S.; Singh, R. B.; Singh, S. P. Characterization of phenolic compounds in some Indian mango cultivars. *Int. J. Food. Sci. Nutr.* **2004**, *55* (2), 163−9.

(4) Zhang, Y.; Qian, Q.; Ge, D.; Li, Y.; Wang, X.; Chen, Q.; Gao, X.; Wang, T. Identification of benzophenone C-glucosides from mango tree leaves and their inhibitory effect on triglyceride accumulation in 3T3-L1 adipocytes. *J. Agric. Food Chem.* **2011**, *59* (21), 11526−33.

(5) Aderibigbe, A. O.; Emudianughe, T. S.; Lawal, B. A. Evaluation of the antidiabetic action of Mangifera indica in mice. *Phytother. Res.* **2001**, *15* (5), 456−8.

(6) Severi, J. A.; Lima, Z. P.; Kushima, H.; Brito, A. R.; Santos, L. C.; Vilegas, W.; Hiruma-Lima, C. A. Polyphenols with antiulcerogenic action from aqueous decoction of mango leaves (Mangifera indica L.). *Molecules* **2009**, *14* (3), 1098−110.

(7) Nkuo-Akenji, T.; Ndip, R.; McThomas, A.; Fru, E. C. Anti-Salmonella activity of medicinal plants from Cameroon. *Cent. Afr. J. Med.* **2001**, *47* (6), 155−8.

(8) Ge, D.; Zhang, Y.; Liu, E.; Wang, T.; Hu, L. Chemical investigation of *Mangifera indica* L. Leaves. *Chin. Herb. Med.* **2011**, *42* (3), 428−431.

(9) Daval, M.; Foufelle, F.; Ferre, P. Functions of AMP-activated protein kinase in adipose tissue. *J. Physiol.* **2006**, *574* (Pt 1), 55−62.

(10) Zhang, B. B.; Zhou, G.; Li, C. AMPK: an emerging drug target for diabetes and the metabolic syndrome. *Cell Metab.* **2009**, *9* (5), 407−16.

(11) Gamble, J.; Lopaschuk, G. D. Insulin inhibition of 5′ adenosine monophosphate-activated protein kinase in the heart results in activation of acetyl coenzyme A carboxylase and inhibition of fatty acid oxidation. *Metabolism* **1997**, *46* (11), 1270−4.

(12) Kola, B.; Grossman, A. B.; Korbonits, M. The role of AMP-activated protein kinase in obesity. *Front. Horm. Res.* **2008**, *36*, 198−211.